Kinetic Modelling of Aqueous Copper (II) Ions Adsorption onto Turmeric Powder: Effect of Temperature

[1]Amtul Qayoom*, [2]Syed Arif Kazmi and [1]Saeeda Nadir Ali
[1]*Department of Chemistry, NED University of Engineering and Technology, Karachi-75270, Pakistan.*
[2]*H.E.J. Research Institute of Chemistry, International Center for Chemical and Biological Sciences University of Karachi, Karachi, Pakistan.*
amtulq@neduet.edu.pk*

(Received on 29th June 2016, accepted in revised form 29th December 2016)

Summary: Turmeric was found to sequester toxic metal ions from their aqueous solutions but thorough understanding of metal-adsorbent interaction requires assessment of adsorption rates. Therefore, in present work reaction and diffusion based kinetic models were applied on adsorption data to evaluate adsorption efficiency of turmeric. The correlation of coefficient, R^2, for linear regression of pseudo second-order and Elovich kinetic models were found to be close to unity indicating that adsorption of aqueous Cu (II) onto turmeric was chemisorption process and its kinetics followed pseudo-second-order and Elovich models. The value of q_e (theoretical) calculated from pseudo-second order model and q_e (experimental) were also close to each other. On raising temperature from 298K to 313K, initial adsorption rate, h_o, increased from 0.0031 to 0.032 gmmol^{-1}min^{-1} and second-order kinetic constant, k_2, increased from 2.74 to 12.27 g mmol^{-1}min^{-1} indicating that Cu (II) adsorption onto turmeric powder is of endothermic nature. On the other hand, Elovich model parameters α (mmol g^{-1} min^{-1}) and β_E (gmmol^{-1}) initially increased and then decreased on raising temperature from 298K to 313K. Intraparticle diffusion plot showed multi-linearity suggesting involvement of two step diffusion process. The presence of pores on adsorbent surface was confirmed by Scanning Electron Micrograph. The value of activation energy was found to be 75.29 kJ mol^{-1}. On the basis of kinetic parameters determined at different temperatures and value of activation energy, chemisorption can be assumed as rate controlling mechanism for aqueous Cu (II) adsorption onto turmeric surface.

Keywords: Copper, Turmeric, Kinetic, Adsorption, Intraparticle Diffusion

Introduction

Copper is one of the vital trace micronutrients which plays important role in the body by acting as a reductant and ligand to many proteins and enzymatic activities [1]. Deficiency of Cu (II) may cause symptoms such as dermatitis, electrolyte-imbalance, gastrointestinal disorders, nausea, anaemia etc [2, 3]. However, excess Cu (II) intake is harmful to human body because of its ability to produce free oxygen radicals and cause DNA damage, skin, brain, heart and pancreas diseases [3].

The use of herbs and medicinal plants as natural heavy metal chelators is well reported [4, 5]. Some dietary fibres such as lignin, pectin and cellulose have also been found to bind metals and decrease their bioavailability in living organisms [6–8]. Milk protein (casein) is also found to exhibit biosorptive properties for toxic metal ions in biosystem [9]. Turmeric (Curcuma longa) is an important medicinal herb in traditional Indo-Pak cuisine. It is frequently used as a spice, preservative, seasoning and colouring agent. Presence of curcuminoids, carbohydrates, proteins etc. suggests its capability to fight metal toxicity by interacting and binding with toxic metals through chemical and/or physical adsorption, ion exchange, complexation, coordination and micro precipitation etc. Lots of scientific and commercial literature also mentioned turmeric as heavy metal chelators and prescribed it for detoxification against heavy metal poisoning but systematic evaluation of its metal scavenging properties is still needed [10–13].

In previous work, effects of varying experimental conditions on aqueous Cu (II) adsorption onto turmeric powder were evaluated. Equilibrium and thermodynamic parameter were also determined [14–17]. Turmeric was found to sequester Cu (II) and Cd (II) ions from aqueous solutions. However, efficiency of sorbents cannot be assessed without studying adsorption kinetics. The application of kinetic models on experimental data and their thorough analysis would be helpful in understanding possible interaction mechanisms between adsorbate and adsorbent surface.

The main objective of present study is to understand adsorption mechanism by applying various reactions and diffusion based kinetic models on experimental data. The relationship between

*To whom all correspondence should be addressed.

temperature and various kinetic parameters is also explored. Outcomes of this study will be helpful in confirming metal chelating capability of turmeric.

Experimental

Adsorbent

Commercially available turmeric powder (Shan food limited, Pakistan) was purchased and used without further purification.

Scanning Electronic Microscopic (SEM) Studies

Adsorbent sample was fixed on a metal stubs and a thin layer of Au was coated on it via vapour deposition. The morphology of the Au coated turmeric powder was investigated by using Scanning Electron Microscope (JSM5910, JEOL, Japan).

Adsorbate Solution

Adsorbate stock solution of copper(II) was prepared by dissolving 0.50 g $CuSO_4.5H_2O$ per liter of deionized water, which was obtained by passing double distilled water through a column of cation exchanger (Amberlite resin IRA-401 from BDH). Dilute solutions of different working standards were prepared from stock solution.

Batch Adsorption Studies

50 mL of metal ion solutions with 0.38-1.51 mmol L^{-1} concentration were placed in specially designed double jacketed 100 mL container with a supply of water circulation at 298-313 K. 0.500 ± 0.001g turmeric powder was added to the solution to obtain a suspension. The suspension was adjusted to pH 6 by adding required volume of 0.1 M HNO_3. A series of such suspensions were stirred at a constant speed at 298-313K. The samples were taken at different time intervals (1–100 min) and contents were suction filtered.

A PerkinElmer Model Analyst 700 atomic absorption spectrophotometer was employed for quantitative analysis of metal ions. The adsorbed metal ions concentration was computed by subtracting final concentration from initial concentration. Batch adsorption tests were conducted in triplicate and average concentration was calculated by taking their mean values.

Metal uptake (q_e) and percent adsorption are determined as follows:

$$q_e = V \times \frac{(C_i - C_e)}{m} \quad (1)$$

$$\% \ adsorption = \frac{C_i - C_t}{C_i} \times 100 \quad (2)$$

where adsorbed Cu (II) ions is represented as q_e (mmol g^{-1}), volume of the sorbate solution as V (L), amount of turmeric powder added as m (g) and Cu (II) ions concentration in the solution in the beginning, at equilibrium and at time t as C_i (mmol L^{-1}), C_e(mmol L^{-1}), C_t (mmol L^{-1}), respectively.

Kinetic Models

Kinetic modelling is one of the key tools to evaluate adsorption mechanism. Kinetic models can be categorized two major classes.

a) Reaction based kinetic models, and
b) Diffusion-based kinetic models.

Reaction-Based Models

Legergren equation for pseudo-first order is given as: [18]

$$\frac{dq_t}{dt} = k_1(q_e - q_t) \quad (3)$$

At the initial conditions q_t = 0 at t = 0, hence, integrating equation (3) results into:

$$\log(q_e - q_t) = \log q_e - \frac{k_1}{2}.303\ t \quad (4)$$

where equilibrium concentration of adsorbed Cu (II) ions is taken as q_e (mmol g^{-1}) and the same at time t (min) is represented as q_t (mmol g^{-1}), respectively and pseudo-first order rate constant as k_1 (min^{-1}). Log (q_e-q_t) was plotted versus t to assess the pseudo-first order kinetic model.

Pseudo-second order model

Equation (5) is used to describe pseudo-second order kinetic model [19]:

$$\frac{dq_t}{d_t} = k_2(q_e - q_t)^2 \quad (5)$$

where pseudo-second order rate constant is represented as k_2 ($gmmol^{-1}min^{-1}$). Rearranging variables and integrating Eq. (4) at q_t = 0 to q_t = q_t and t = 0 to t = t gives following equation.

$$\frac{1}{(q_e - q_t)} = \frac{1}{q_e} + k_2 t \quad (6)$$

Linearizing Eq. (5) results in:

$$\frac{t}{q_t} = \frac{1}{k_2 q_e^2} + \frac{t}{q_e} \quad (7)$$

Eq. (7) results in straight line when t/q_t is plotted versus t. Slope and intercept of the plot were used to estimate values of parameters, q_e and k_2, respectively. Initial sorption rate h_o (mmol g^{-1} min^{-1}) was determined from the value of rate constant (k_2) using Eq. (8)

$$h_o = k_2 q_e^2 \quad (8)$$

Elovich Model

Elovich equation explains 2nd order kinetics by considering actual adsorbent surfaces as energetically heterogeneous [20]. Eq. (9) represents Elovich equation [21]:

$$\frac{dq_t}{dt} = \alpha \exp(-\beta_E q_t) \quad (9)$$

where initial adsorption rate (mmol g^{-1} min^{-1}) is represented as α, and β_E is associated with the activation energy for chemisorption and degree of surface coverage (g $mmol^{-1}$). Assuming that $\alpha\ \beta_E\ t >> 1$ and $q_t = 0$ at t = 0, Elvoich equation is simplified as follows:

$$q_t = \frac{1}{\beta_E} \ln(\alpha\beta_E) + \beta_E \ln t \quad (10)$$

Plot of q_t versus lnt is used to assess validity of Elovich equation. If a straight line is obtained, intercept and slope of the line are used to estimate α and β_E, respectively. If Elovich equation is valid, it favours the assumption that adsorption rate can be described by chemisorption mechanism [22].

Diffusion-Based Model

Adsorption kinetics depends on various independent processes occurring simultaneously or in series. Usually adsorbate uptake on porous adsorbents occurs in following four steps [23].

- Bulk diffusion: movement of sorbate from bulk solution to the boundary layer at liquid-sorbent junction.
- Film diffusion: adsorbate transfer from the boundary layer to the external adsorbent surface.
- Intraparticular diffusion: surface diffusion and/or pore diffusion of sorbate from the external adsorbent surface to the intraparticular active sites.
- Sorbate uptake by the active sites present on adsorbent surface.

Adsorption rate may depend on one or more of these steps. Usually bulk diffusion and sorbate adsorption on adsorbent surface is rapid and does not influence overall kinetics of adsorption [24]. Film diffusion and intraparticle diffusion act in parallel and slowest of these steps will govern overall sorption rate. Though, the rate-determining step might be distributed between external transport and intraparticle diffusion.

Intraparticle diffusion (Weber–Morris model)

If adsorption rate is determined by intra-particle diffusion step, adsorbion is directly related to the square root of contact time. Therefore, adsorption capacities as a function of $t^{1/2}$ were employed to calculate adsorption rates. Following equation represents Weber and Morris Intraparticle diffusion model [25]:

$$q_t = k_i \sqrt{t} + C \quad (11)$$

where intraparticle diffusion constant is represented by k_i and C gives an idea of the degree of the boundary layer thickness.

Activation Energy

Arrhenius equation was used to calculate activaton of Cu (II) ions:

$$\ln k_2 = \ln k_o - \frac{E_A}{RT} \quad (12)$$

where second-order adsorption rate constant (g $mmol^{-1}s^{-1}$) is represented as k_2, activation energy (J mol^{-1}) as E_A, Arrhenius factor (g $mmol^{-1}$ s^{-1}) as k_0, gas constant (J K^{-1} $mmol^{-1}$) and temperature (K) of adsorbate solution as R and T, respectively.

Result and Discussion

Scanning Electronic Microscopic (SEM) Studies

Scanning Electron Micrograph of turmeric powder was taken at X35, 000 magnification to

observe morphology of turmeric surface (Fig. 1). SEM image shows that a large number of pores with heterogeneous sizes and shapes are present on adsorbent surface. Their presence on adsorbent surface is indicative of its good adsorption ability because porosity of adsorbent surface increases its surface area and available binding sites for adsorbate ions.

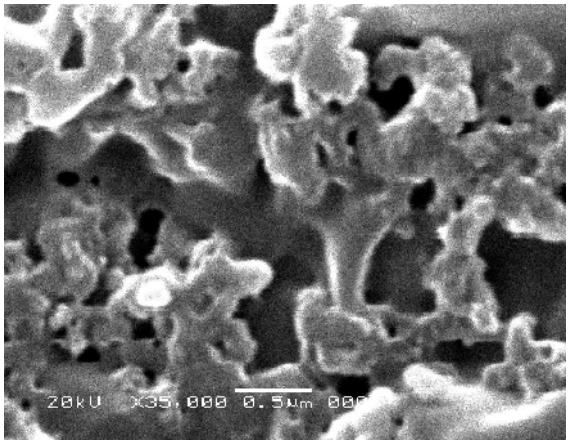

Fig. 1: SEM micrograh of turmeric powder with magnification of X35,000 showing presence of pores on its surface.

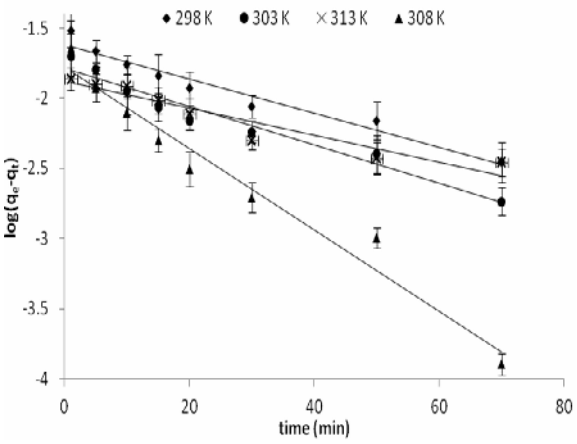

Fig. 2: Plot of the linearized pseudo-first order kinetic equation for the adsorption of Cu (II) onto turmeric powder at 298-313K. Initial pH 6(±0.1), turmeric dose 10 g L^{-1}, [Cu (II)] 0.67 mmol L^{-1}. Solid lines represent best fit for linear regression of the adsorption data. Error bars indicate ±one standard deviation of triplicate [Cu(II)] measurement.

Reaction-Based Models

Fig. 2-4 represent the kinetic model plots of experimental data for aqueous Cu (II) adsorption onto turmeric at 298-313K. Resulting kinetic parameters are given in Table-1.

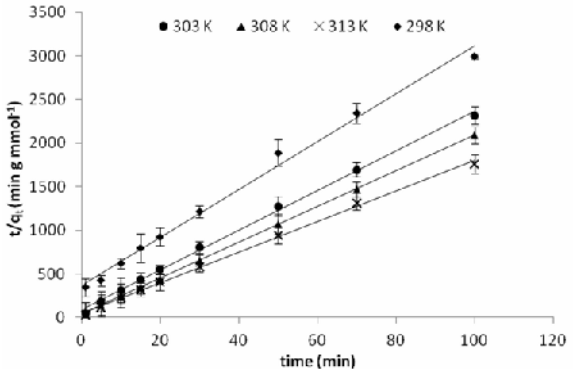

Fig. 3: Plot of the linearized pseudo-second order equation for kinetics of Cu (II) adsorption onto turmeric powder at 298-313K. Initial pH 6(±0.1), turmeric dose 10 g L^{-1}, [Cu (II)] 0.67 mmol L^{-1}. Solid lines represent best fit for linear regression of the adsorption data. Error bars indicate ±one standard deviation of triplicate [Cu (II)] measurement.

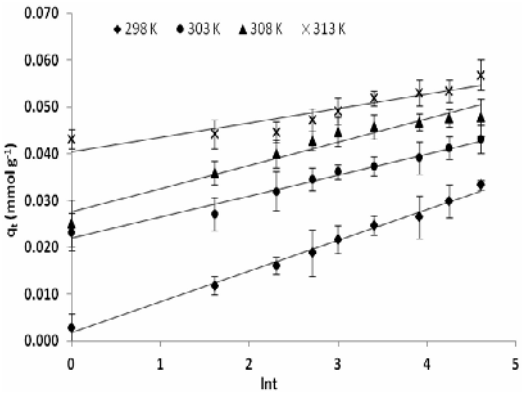

Fig. 4: Plot of the linearized Elovich equation for the adsorption of Cu(II) onto turmeric powder at 298-313K. Initial pH 6(±0.1), turmeric dose 10 g L-1, [Cu (II)] 0.67 mmol L-1. Solid lines represent best fit for linear regression of the adsorption data. Error bars indicate ±one standard deviation of triplicate [Cu (II)] measurement.

Table-**Error! Style not defined.**.

Kinetic Model	Temp. (K)	298	303	310	313
Pseudo-first order	Q_e (mmol g^{-1}) (exp)	0.033	0.043	0.047	0.054
	Q_e (mmol g^{-1})	0.024	0.016	0.017	0.015
	k_1 (min^{-1})	0.027	0.03	0.067	0.021
	R^2	0.95	0.95	0.96	0.88
Pseudo-second order	Q_e (mmol g^{-1})	0.034	0.042	0.049	0.054
	k_2 (g $mmol^{-1}$ min^{-1})	2.74	8.54	11.83	12.27
	h_o(mmol g^{-1} min^{-1})	0.0031	0.015	0.028	0.032
	R^2	0.99	0.99	0.99	0.99
Elovich	α (mmol g^{-1} min^{-1})	0.0087	0.59	1.22	0.82
	β (g $mmol^{-1}$)	151.51	222.22	200	166.66
	R^2	0.99	0.97	0.94	0.92
Intraparticle diffusion	K_{i1}($x10^3$)	1.8	1.39	2.4	0.54
	C	0.0049	0.024	0.027	0.043
	R^2	0.90	0.96	0.87	0.88
	K_{i2}($x10^3$)	0.26	0.17	0.075	0.17

Linear correlation coefficients obtained by applying pseudo-first order model were low and theoretical and experimental q_e values were different. Therefore, aqueous Cu (II) adsorption onto turmeric was not governed by pseudo-first order mechanism. Pseudo-second order kinetic model provided better fit. This model assumes that aqueous Cu (II) adsorption onto turmeric followed a second order mechanism and the metal uptake rate decreased with time because of increasing occupancy of available binding sites. Moreover, Elovich equation was also applied on experimental data to describe second order kinetics. The theoretical and experimental values of q_e calculated from pseudo-second order model were quite similar and coefficient of correlation for pseudo-second order kinetic and Elovich kinetic models were high, suggesting chemical adsorption as rate limiting step. This result was anticipated because due to the presence of curcuminiods, carbohydrates and proteins, turmeric surface acts as a chelate exchanger. Therefore, adsorption of Cu (II) onto turmeric powder obeyed Elovich and second-order kinetic model. When temperature was raised from 298K to 313K, initial adsorption rate increased from 0.0031to 0.032 g $mmol^{-1}$ min^{-1} and rate constant increased from 2.74 to 12.27 g $mmol^{-1}$ min^{-1} indicating Cu (II) adsorption onto turmeric powder as of endothermic nature.

Intraparticle Diffusion

In Fig. 5, values of q_t are plotted versus $t^{1/2}$ to evaluate intraparticle diffusion parameters for aqueous Cu (II) adsorption onto turmeric powder. Intraparticle diffusion plot showed two linear regions with different slopes. This kind of multlinearity in intraparticle diffiusion curve is also observed for adsorption of aqueous copper ions by other adsorbents and this phenomenon have been described as macro and micropore diffusion in many recent research publications [26–30]. Thus it can be assumed that at least two steps were involved in the intraparticle diffusion process; first linear portion can be ascribed to adsorbate diffusion from the solution to easily accessible binding sites on external surface of adsorbate while second linear region showed adsorbate diffusion to less accessible internal pores until equilibrium was reached.

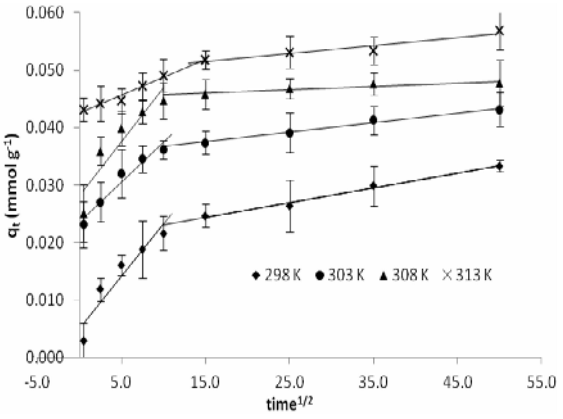

Fig. 5: Plot of the Intraparticle diffusion equation for the adsorption of Cu(II) onto turmeric powder at 298-313K. Initial pH 6(±0.1), turmeric dose 10 g L^{-1}, [Cu (II)] 0.67 mmol L^{-1}. Solid lines represent best fit for linear regression of the adsorption data. Error bars indicate ±one standard deviation of triplicate [Cu (II)] measurement.

Slope of first linear region was attributed to diffusion rate of surface adsorption, k_{i1}(mmol g^{-1} min^{-0}). Higher k_{i1} suggested that surface adsorption was rapid and hence not rate limiting step. The k_{i2} (mmol g^{-1} $min^{-0.5}$) represented slope of second linear region in the plot and it had been taken as the intraparticle diffusion constant. The intercept of the first linear part, C, was taken as the boundary layer thickness. Value of the intercept suggest role of surface adsorption in rate-limiting step [30]. Initially, Cu (II) ions uptake by the exterior surface of turmeric powder was rapid. Followed by saturation of exterior

surface, the Cu (II) ions were adsorbed by the interior particle surfaces by entering into the adsorbent particles through the pores within the particles. Gradually, the diffusion rate became slower with decrease in the adsorbate concentration and eventually diffusion equilibrium was attained. Low k_{i2} values suggested that adsorption of aqueous Cu (II) onto turmeric is basically governed by intraparticle diffusion but plot of intraparticle diffusion plot did not yield a straight line crossing the origin. Therefore Cu (II) adsorption onto turmeric powder is not entirely controlled by pore diffusion [31].

Activation Energy

The activation energy, determined from slope of $\ln k_2$ versus 1/T plot was found to be 75.29 kJ mol^{-1} for Cu (II) adsorption onto turmeric powder. Values of activation energy are useful in providing information about types of sorption i.e. physical or chemical. Activation energies less than 40 kJ mol^{-1} are usually indicative of physisorption while higher than 40 kJ mol^{-1} values are associated with chemisorption [32]. Increase in Cu (II) adsorption onto turmeric powder on raising temperature indicated that it is endothermic process. Activation energy higher than 40 kJ mol^{-1} was suggestive of chemisorption as considerable and rate controlling step for aqueous Cu (II) adsorption onto turmeric surface.

Conclusion

Present work was aimed to understand kinetics mechanism of the adsorption of aqueous Cu (II) onto turmeric as it would be useful in determination and evaluation of turmeric's adsorption efficiency. Various reaction and diffusion based models were applied on experimental data. It was found that aqueous Cu (II) adsorption onto turmeric followed pseudo-second order and Elovich kinetic models. Moreover, the values of activation energies for adsorption of aqueous Cu (II) onto turmeric were also determined using slope of the $\ln k_2$ versus 1/T plot, which was found to be 83.28 kJ mol^{-1}. Therefore it is concluded that the adsorption of aqueous Cu (II) onto turmeric is basically chemisorption phenomenon. Further investigation on identifying responsible constituent of turmeric for sequestration of copper ions from aqueous solutions is highly recommended. This may involve chemically stripping turmeric with various solvents and studying adsorbing abilities of residual solid matrix.

References

1. J. H. Kaplan and E. B. Maryon, How Mammalian Cells Acquire Copper: An Essential but Potentially Toxic Metal, *Biophys. J.*, **110**, 7 (2016).
2. M. E. Shils and M. Shike, Modern Nutrition in Health and Disease. Lippincott Williams & Wilkins, p. 295 (2006).
3. P. A. Balch, Prescription for Nutritional Healing. Avery, p.339, (2006).
4. P. Y. Y. Wong and D. D. Kitts, Studies on the Dual Antioxidant and Antibacterial Properties of Parsley (*Petroselinum crispum*) and cilantro (*Coriandrum sativum*) Extracts, *Food Chem.*, **97**, 505 (2006).
5. Z. R. Komy, Determination of Acidic Sites and Binding Toxic Metal Ions on Cumin Surface Using Nonideal Competitive Adsorption Model, *J Colloid Interface Sci*, **270**, 281 (2004).
6. W. Zhang, L. Y. Zhang, X. J. Zhao and Z. Zhou, Citrus Pectin Derived Porous Carbons as a Superior Adsorbent Toward Removal of Methylene Blue, *J. Solid State Chem.*, **243**, 101 (2016).
7. M. Zhang, L. H. Xu, S. S. Lee and Y. S. Ok, Sorption of Polycyclic Aromatic Hydrocarbons (PAHs) by Dietary Fiber Extracted from Wheat Bran, *Chem. Speciat. Bioavailab.*, **28**, 13 (2016).
8. P. Manini, L. Panzella, T. Eidenberger, A. Giarra, P. Cerruti, M. Trifuoggi and A. Napolitano, Efficient Binding of Heavy Metals by Black Sesame Pigment: Toward Innovative Dietary Strategies to Prevent Bioaccumulation, *J. Agric. Food Chem.*, **64**, 890 (2016).
9. S. P. Mishra, D. Tiwari, R. S. Dubey and M. Mishra, Biosorptive Behaviour of Casein for Zn^{2+}, Hg^{2+} and Cr^{3+}: Effects of Physico-Chemical Treatments, *Bioresour. Technol.*, **63**, 1 (1998).
10. A. A. Farooqui, Therapeutic Potentials of Curcumin for Alzheimer Disease. Springer International Publishing, p.114 (2016).
11. J. Wignall, Raw and Simple Detox: A Delicious Body Reboot for Health, Energy, and Weight Loss. Quarry Books, p.310 (2015).
12. W. R. García-Niño and J. Pedraza-Chaverrí, Protective Effect of Curcumin Against Heavy Metals-Induced Liver Damage, *Food Chem. Toxicol.*, **69**, 182 (2014).
13. S. C. Lawton, Asperger Syndrome: Natural Steps Toward a Better Life. Praeger Publishers, p.114, (2007).
14. A. Qayoom, S. A. Kazmi, and Naushaba-Rafiq, Removal of Cu (II) Ions from Aqueous Solutions by Turmeric Powder, *J. Chem. Soc. Pak.*, **31,** 876(2009).

15. A. Qayoom, S. A. Kazmi, S. N. Ali, and B. Sciences, Adsorption of Aqueous Cd (II) Ions onto Turmeric Powder, **28**, *Sci. int*, 3777 (2016).
16. A. Qayoom and S. A. Kazmi, Effect of Temperature on Equilibrium and Thermodynamic Parameters of Cd (II) Adsorption onto Turmeric Powder, *J. Chem. Soc. Pakistan*, **34**, 1084 (2012).
17. A. Qayoom and S. A. Kazmi, "Effect of Temperature on Sequestration of Cu(II) from Aqueous Solution onto Turmeric Powder, *J. Chem. Soc. Pak. Soc.*, **32**, 582 (2010).
18. S. Lagergren, About the Theory of So-Called Adsorption of Soluble Substances, *K. Sven. Vetenskapsakademiens. Handl.*, **24**, 1(1898).
19. Y. S. Ho and G. McKay, Sorption of Dye From Aqueous Solution by Peat, *Chem. Eng. J.*, **70**, 115 (1998).
20. M. K. Aroua, S. P. P. Leong, L. Y. Teo, C. Y. Yin, and W. M. A. W. Daud, Real-Time Determination of Kinetics of Adsorption of lead(II) onto Palm Shell-Based Activated Carbon Using Ion Selective Electrode, *Bioresour. Technol.*, **99**, 5786 (2008).
21. C. Aharoni and M. Ungarish, Kinetics of Activated Chemisorptions. Part I: the Non-Elovichian part of the Isotherm., *J. Chem. Soc. Faraday Trans.*, **72**, 265 (1976).
22. M. Dávila-Estrada, J. J. Ramírez-García, M. C. Díaz-Nava, and M. Solache-Ríos, Sorption of 17α-Ethinylestradiol by Surfactant-Modified Zeolite-Rich Tuff from Aqueous Solutions, *Water, Air, & Soil Pollut.*, **227**, 1 (2016).
23. A. R. Cestari, E. F. S. Vieira, A. A. Pinto, and E. C. N. Lopes, Multistep Adsorption of Anionic Dyes on Silica/Chitosan Hybrid. 1. Comparative Kinetic Data From Liquid- and Solid-Phase Models., *J. Colloid Interface Sci.*, **292**, 363 (2005).
24. S. Afroze, T. K. Sen, and H. M. Ang, Adsorption Removal of Zinc (II) from Aqueous Phase by Raw and Base Modified Eucalyptus Sheathiana Bark: Kinetics, Mechanism and Equilibrium Study, *Process Saf. Environ. Prot.*, **102**, 336 (2016).
25. Walter J. Weber and J. C. Morris, Kinetics of Adsorption on Carbon from Solution, *J. Sanit. Eng. Div.*, **89**, 31 (1963).
26. H. Zare, H. Heydarzade, M. Rahimnejad, A. Tardast, M. Seyfi, and S. M. Peyghambarzadeh, Dried Activated Sludge as an Appropriate Biosorbent for Removal of Copper (II) Ions, *Arab. J. Chem.*, **8**, 858 (2015).
27. A. E. Ofomaja, E. B. Naidoo and S. J. Modise, Dynamic Studies and Pseudo-Second Order Modeling of Copper(II) Biosorption onto Pine Cone Powder, *Desalination*, **251**, 112 (2010).
28. A. E. Ofomaja, Biosorption Studies of Cu(II) onto Mansonia Sawdust: Process Design to Minimize Biosorbent Dose and Contact Time, *React. Funct. Polym.*, **70**, 879 (2010).
29. H. Benaïssa and M. A. Elouchdi, Biosorption of Copper (II) Ions from Synthetic Aqueous Solutions by Drying Bed Activated Sludge, *J. Hazard. Mater.*, **194**, 69 (2011).
30. A. S. Ozcan and A. Ozcan, Adsorption of Acid Dyes from Aqueous Solutions onto Acid-Activated Bentonite., *J. Colloid Interface Sci.*, **276**, 39 (2004).
31. G. C. Chen, X. Q. Shan, Y. Q. Zhou, X. Shen, H. L. Huang, and S. U. Khan, Adsorption Kinetics, Isotherms and Thermodynamics of Atrazine on Surface Oxidized Multiwalled Carbon Nanotubes, *J. Hazard. Mater*, **169**, 912 (2009).
32. T. A. Saleh, Isotherm, Kinetic, and Thermodynamic Studies on Hg(II) Adsorption from Aqueous Solution by Silica- Multiwall Carbon Nanotubes, *Environ. Sci. Pollut. Res.*, **22**, 16721 (2015).